A dipolar gas of ultracold molecules

K.-K. Ni, S. Ospelkaus, D. J. Nesbitt, J. Ye* and D. S. Jin*

Received 16th June 2009, Accepted 28th July 2009
First published as an Advance Article on the web 25th August 2009
DOI: 10.1039/b911779b

Ultracold polar molecular gases promise new directions and exciting applications in collisions and chemical reactions at ultralow energies, precision measurements, novel quantum phase transitions, and quantum information science. Here we briefly discuss key experimental requirements for observing strong dipole–dipole interactions in an ultracold dipolar gas of molecules. We then survey current experimental progress in the field with a focus on our recent work creating a near quantum degenerate gas of KRb polar molecules [Ni *et al.*, *Science*, 2008, **322**, 231].

I. Introduction

Ultracold atomic gases (with temperatures below 1 μK) have provided many exciting and diverse applications in the physical sciences, including improvements in neutral atomic clocks, precision tests of fundamental physics, novel sensors of tiny forces, as well as new architectures for quantum information and computing. These systems are miniature laboratories for studying ultracold collisions, resonances, and few-body physics, and, in addition, provide model systems where one can explore many-body quantum phenomena such as Bose condensation, superfluidity, and Fermi superfluidity (the electrically neutral analog of superconductivity). The underlying basis for these many uses is that ultracold atomic gases can be trapped, interrogated for long times, and precisely controlled at the quantum level, in both the atoms' internal (*i.e.*, electronic, fine, and hyperfine) and external (*i.e.*, motional state in the lab frame) degrees of freedom. As will be explored in this perspective, extending this type of control to an ultracold gas of polar molecules would open exciting new research directions because of the richer energy level structure of molecules, the relatively strong and long-range electric dipole–dipole interaction between polar molecules, and the intriguing possibility for studies of chemically reactive collisions.

The focus of this work will be on ultracold polar species, the simplest of which are heteronuclear diatomic molecules. However, even diatomic molecules have a considerably more complicated energy level structure than atoms due to the additional rotational and vibrational degrees of freedom. This has made laser based cooling into the ultracold temperature regime a major technical hurdle. Nevertheless, obtaining such a class of ultracold polar molecules would open new possibilities

JILA, National Institute of Standards and Technology and University of Colorado, Department of Physics, University of Colorado, Boulder, CO 80309-0440, USA. E-mail: junye@jilau1.colorado.edu, jin@jilau1.colorado.edu

Kang-Kuen Ni obtained her BS from the University of California, Santa Barbara in 2003. She is a recipient of an NSF Graduate Fellowship and is currently pursuing her PhD in physics at the University of Colorado, Boulder.

Silke Ospelkaus obtained her diploma in physics from the University of Bonn and her PhD from the University of Hamburg in 2006. Her PhD work was awarded the AMOP thesis prize from the German Physical Society. Since 2007, she works as a postdoctoral research associate and Feodor-Lynen Fellow of the Alexander von Humboldt Foundation at JILA, Boulder.

David Nesbitt is a NIST Fellow, Fellow of the American Physical Society, Fellow of the Royal Society of Chemistry and Adjoint Professor in the Department of Chemistry and Biochemistry at the University of Colorado. Research interests at JILA involve high resolution laser techniques to study transient radicals and molecular ions, quantum state-resolved inelastic/reactive scattering at gas–liquid interfaces, and single molecular fluorescence dynamics of plasmonic nanostructures, quantum dots, and RNA biopolymers. Honors include the Wilson Prize, Arthur S. Flemming Award, Edward Uhler Condon Award, Earle K. Plyler Prize, William F. Meggers Award, and the Alexander von Humboldt Senior Scientist Award.

Jun Ye is a Fellow of JILA and an Adjoint Professor of Physics at the University of Colorado. He is also a Fellow of NIST, of the American Physical Society, and of the Optical Society of America. Research interests include precision measurement and quantum metrology, ultracold atoms and molecules, and ultrafast science and quantum control. He has co-authored over 200 technical papers and has delivered 250 invited talks. Honors include I. I. Rabi Prize, Carl Zeiss Award, William F. Meggers Award, Adolph Lomb Medal, Arthur S. Flemming Award, Presidential Early Career Award, US Commerce Department group Gold Medal, Friedrich Wilhem Bessel Award, Samuel Wesley Stratton Award.

Deborah Jin is a NIST Fellow and an Adjoint Professor of Physics at the University of Colorado. Her current experimental research at JILA includes studies of ultracold Fermi gases and the BCS–BEC crossover, ultracold polar molecules, strongly interacting Bose–Einstein condensates, and Bose–Fermi gas mixtures. She is a Fellow of the National Academy of Sciences, the American Association for the Advancement of Science, and the American Physical Society. Honors include a MacArthur fellowship, the Benjamin Franklin Medal in Physics, and Sigma Xi's William Proctor Prize for Scientific Achievement.

for precision measurements.[1–3] One example is the search for a permanent electric dipole moment of the electron, where polar molecules can provide much larger internal electric fields than could be directly applied to electrons in the lab or inside an atom. The more complex internal states of polar molecules will also enable the development of new tools for controlling and manipulating ultracold gases. In the area of ultracold collisions, polar molecule gases offer electric-field tuning of interactions,[4] access to new types of resonances,[5] and ultracold chemistry.[6] For quantum information applications, the relatively strong dipole–dipole interaction, which can be switched on and off on demand with an applied external electric field, offers a means for controlled creation of entangled states.[7–9] The dipole–dipole interaction, which is long-range as opposed to the much more highly localized contact interaction of ultracold atoms, could also be exploited in quantum gases of polar molecules to realize novel phases of matter.[10–12]

Realizing an ultracold gas of polar molecules has been challenging, in a large part because of the same complex internal state structure that makes them interesting. This perspective will discuss experimental efforts to create gases of ultracold polar molecules, with a focus on our recent success in creating a near quantum degenerate gas of polar molecules.[13] However, before discussing the experiments, it is useful to consider what is required for proposed applications of an ultracold gas of polar molecules.

II. Dipole–dipole interaction

The relatively large dipole–dipole interaction between polar molecules is a key ingredient for many proposed uses for ultracold polar molecules. Interestingly, for the goal of studying novel phases of a dipolar quantum gas, the specific chemical nature of molecules is typically not critical, but having a permanent electric dipole moment is essential. In SI units, the dipole–dipole interaction has the form $\frac{\vec{d}_1\cdot\vec{d}_2-3(\vec{d}_1\cdot\hat{r})(\vec{d}_2\cdot\hat{r})}{4\pi\varepsilon_0 r^3}$, where $\vec{d}_1$ and $\vec{d}_2$ are the two dipole moments, ε_0 is the permittivity of vacuum, and $\vec{r}$ is the separation between the two dipoles. The dipole–dipole interaction has two features that are very different from typical interactions between ultracold atoms. First, the dipole–dipole interaction falls off as $1/r^3$ and therefore predominates at long-range. In contrast, typical chemical bonding (exponential) and even dispersive van der Waals forces ($1/r^6$) are short range in comparison with the large de Broglie wavelengths realized for ultracold atoms or molecules. In fact, the interparticle potentials between atoms and/or non-polar molecules can be adequately described as a so-called ''contact interaction'', which (with apologies to the richness of chemistry) can to an excellent approximation be simply treated as a delta-function! Second, the dipole–dipole interaction is spatially anisotropic, and, as can be seen from the expression above, the interaction can be either attractive or repulsive depending on the orientation of the two dipoles with respect to the intermolecular displacement, $\vec{r}$. In contrast, the interaction between atoms at ultracold temperatures is typically limited by finite angular momentum barriers to spatially isotropic s-wave interactions, *i.e.* where the relative orbital angular momentum is zero. This special property of polar molecules permits the experimentalists to control the relative spatial orientation, and thereby tune the intermolecular interaction by uses of external electric fields.

Samples of ultracold gases with dipole–dipole interactions have been realized using chromium atoms in a Bose–Einstein condensate.[14] Chromium has an exceptionally large magnetic dipole moment of $6\mu_b$, where μ_b is the Bohr magneton. In these pioneering experiments, the anisotropic character of the dipole–dipole interaction has been beautifully revealed.[14–16] One of the key advantages of polar molecules is that the electric dipolar interaction can be much stronger. For example, the interaction between two polar molecules with a typical electric dipole moment of order of a Debye, where $1\ \mathrm{D} = 3.34 \times 10^{-30}$ C m, is approximately equal to the interaction between magnetic dipoles with a dipole moment of $100\mu_b$. These much stronger interactions will in particular allow the long-range character ($1/r^3$) of the dipolar interaction to be manifested in experiments. This long-range nature of the dipole–dipole interaction is exploited in proposals aimed at realizing new types of many-body Hamiltonians and novel phases of matter with ultracold polar molecules. A review of theoretical work on this subject can be found in ref. 10.

It is convenient to have a length scale that describes the range of interparticle separations over which the dipolar interaction plays an important role. Similar to the case of the van der Waals length defined for the interaction of neutral atoms,[17] Bohn *et al.*[18] have defined a characteristic dipole length given by $l_D = Md^2/(4\pi\varepsilon_0\hbar^2)$, where M is the reduced mass, d is the dipole moment of the molecules, and $\hbar$ is Planck's constant divided by 2π. The dipole length is essentially a measure of the intermolecular separation at which the dipole–dipole interaction energy equals the kinetic energy that corresponds to a de Broglie wavelength at that separation. To get appreciable long-range interactions in a gas of polar molecules, we want l_D to be comparable or greater than the average interparticle spacing. For atoms interacting *via* magnetic dipoles, this dipole length is typically on the order of a few tens of Bohr radii, a_0, or less. For example, Rb with a magnetic dipole moment of $1\mu_b$ has a dipole length of $l_D \approx 1a_0 \simeq 5 \times 10^{-11}$ m, while Cr with a magnetic dipole moment of $6\mu_b$ has $l_D \approx 23a_0$. This is more than 100-fold smaller than the mean interparticle distance even in ultracold atomic gas samples at the highest achievable densities (n) obtained thus far, for which $n^{-1/3} \approx 5000$ to $20\,000a_0$. For polar molecules interacting *via* electric dipoles, however, this length scale can be as large as 10^4 to 10^6a_0, and therefore could be comparable to or even much larger than the interparticle spacing in an ultracold gas. For example, KRb with a dipole moment of 0.566 D has a dipole length l_D of $6000a_0$, while LiCs with a dipole moment of 5.5 D has $l_D = 6 \times 10^5a_0$. In addition, the complex internal structure of molecules offers unique possibilities for shielding and controlling molecular interactions by means of AC and DC electric fields.[19]

To observe dipole–dipole interactions in an ultracold gas of polar molecules, we must consider both two-body and many-body effects. Two-body effects are due to processes where one needs only consider two molecules interacting with each other in isolation. These include, for example, ultracold collisions and ultracold chemistry, where the process can be treated to a

good approximation as bimolecular. Here, the fact that the gas is actually made up of many molecules simply enhances the observed total rate of these processes. In contrast, many-body effects are those that are not simply the sum of two-body processes. One example is the mean-field energy of a dipolar Bose–Einstein condensate.[20] In general, observing many-body effects will likely require a quantum degenerate sample of polar molecules, such as a Bose–Einstein condensate or a quantum degenerate Fermi gas (see section II.B.)

A Ultracold collisions of dipoles

Collisions in the ultracold regime have a number of novel features. With their low energies and long interaction times, ultracold collisions are sensitive probes of the interaction potential and can often be controlled with the application of modest external fields. In addition, the quantum statistics of the colliding particles, for example that of identical fermions or identical bosons, can play an important role. However, molecular gases introduce a completely new type of ultracold collision, namely chemically reactive collisions. Furthermore, polar molecules offer the unique possibility for electric-field control of collisions, as will be described more below. Understanding these two-body processes will be important for exploring many-body phenomena in ultracold gases of polar molecules.

For a given collision energy, interparticle collisions classically occur over a range of impact parameters with corresponding angular momentum barriers. For atoms, the ultracold temperature regime is often characterized by the requirement that collisions occur in only one angular momentum partial wave, namely the s-wave, the only one for which no centrifugal barrier exists. Similarly, for molecules, the ultracold regime can be defined by requiring that only s-wave collisions occur when there is no external electric field. This requirement means that collision energies in the gas should be much less than the height of the p-wave centrifugal barrier, which is, for example, $E/k_B \approx 16$ μK[21] for KRb molecules, where k_B is the Boltzmann constant. In the presence of an external electric field, however, the molecules will tend to polarize and the dipole–dipole interaction becomes important. This has the effect of mixing different angular momentum partial waves; thus even though ultracold collisions may occur in a single scattering channel, that channel can no longer be simply described by a single partial wave.

The long-range nature of the interaction between polar molecules gives rise to a very different and fascinating temperature dependence of ultracold collisions for polar molecules compared to neutral atoms. For species with a short-range potential (*cf.*, delta-function approximation for ultracold atom–atom potentials), the elastic collision cross section becomes a constant, independent of temperature in the ultracold regime. This threshold regime of temperature-independent elastic scattering cross section occurs only when the range of the interaction is much smaller than the inverse scattering wavevector, $1/k$. As discussed above, for dipole–dipole scattering, the range of the interaction can be characterized by a dipole length, l_D.[18] The threshold regime for scattering then occurs only when $l_D < 1/k$, which means that the relative kinetic energy of two colliding molecules is less than $E_D = \hbar^6(4\pi\varepsilon_0)^2/(M^3d^4)$. For fully polarized KRb, for example, this threshold regime corresponds to a temperature of order 80 nK or below, while for LiCs, $E_D/k_B \approx 7$ pK. The important consequence is that for temperatures higher than E_D/k_B, the elastic scattering cross section will be $\sigma = 8\pi l_D/(3k)$ and therefore increasing with decreasing temperature as $T^{-1/2}$.[18] This corresponds to a rate constant for elastic collisions of $k_{elastic} = \sigma v = 8\pi l_D\hbar/(3M)$, which for KRb with a dipole moment of 0.566 D would yield $k_{elastic} \approx 2.5 \times 10^{-9}$ cm^3 s^{-1} independent of the temperature down to 80 nK. Stated more dramatically, polar KRb molecules at 80 nK are predicted to have elastic cross sections on the order of $\sigma \approx 5 \times 10^7$ Å^2.

We can now consider a question relevant to future experiments on cold or ultracold gases of polar molecules, namely what is the density required to observe elastic dipole–dipole collisions? To be experimentally sensitive to collisional effects, such as loss of trapped molecules for inelastic collisions or rethermalization of the gas for elastic collisions, requires that the typical time between collisions, given by the reciprocal collision rate, is less than the interrogation time. Therefore, if we have a time of 1 s to observe a trapped sample of polar molecules with a dipole moment of 1 D, $k_{elastic} \approx 8 \times 10^{-9}$ cm^3 s^{-1} and this prediction implies a minimum number density of about $n \approx 2 \times 10^8$ cm^{-3} is required to observe elastic dipole–dipole collisions. A summary of current experimental achievable numbers can be found in Table 1 in section III.

For any specific experiment, moreover, other important considerations will include the effects of quantum statistics, contributions from the short-range part of the scattering potential, and the possibility of scattering resonances,[4,5] which can further increase these collision rates by orders of magnitude. Fig. 1 shows an example of scattering resonances seen in the predicted electric-field dependent cross section for bosonic polar molecules.[22] These resonances arise from bound states supported by the strong attractive interaction between two molecules, whose energies can therefore be tuned with an applied electric field. These resonances can clearly have a

Table 1 Summary of experimental results for production of cold and ultracold polar molecules. Selected examples of the molecule species with its electric dipole moment (calculated or measured) and the achieved gas temperature, trapped number density and phase-space density are given

Method	Species (dipole/D)	T	Trapped density/cm^{-3}	PSD	Ref.
Buffer gas cooling	NH (1.39)	550 mK	10^8	10^{-14}	34
Stark deceleration	OH (1.67)	50 mK	10^6–10^7	10^{-13}	37 and 38
Photo-association (incoherent)	RbCs (1.3)	100 μK	10^4 (not trapped)	10^{-14}	52
	LiCs (5.5)	260 μK	10^3 (not trapped)	10^{-15}	56
Coherent population transfer starting from Feshbach molecules	KRb (0.566)	350 nK	10^{12}	0.02	13

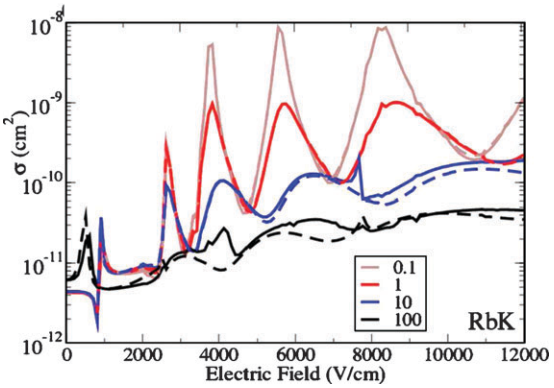

Fig. 1 Elastic dipole scattering resonances. An example of electric-field controlled elastic collision cross section for bosonic polar molecules at a temperature of 0.1, 1, 10 and 100 μK. These potential resonances arise from bound states supported by the attractive dipolar interaction between two molecules. The resonant cross sections increase by orders of magnitude as the temperature is lowered. Adapted with permission from C. Ticknor, *Phys. Rev. A*, 2007, **76**, 052703. Copyright 2007, American Physical Society.

dramatic impact on the elastic collision cross section for an ultracold gas of polar molecules. Additionally, although we have focused in the above discussion on elastic processes, it will also be important and interesting to investigate inelastic collisions,[23] which will determine the lifetime of trapped samples of polar molecules. Indeed, chemically reactive collisions between polar molecules (or between polar molecules and atoms) represent a particularly intriguing new frontier of encounters to be explored in the ultralow temperature regime. By detecting inelastic, or reactive, scattering through trap loss measurements, one can explore how these processes depend on temperature, electric field, quantum statistics, the internal state of the trapped molecules, and the geometry, or dimensionality, of the trapping potential.

B Dipolar quantum gas

Ultracold gases can be used to realize interesting many-body quantum systems where the interactions between particles, along with particles' quantum statistics, govern the macroscopic behavior of the system. In an ultracold gas of polar molecules, the interparticle interactions are relatively strong, spatially anisotropic, and long-range. Proposals taking advantage of these interactions include studies of Bose–Einstein condensates or Fermi gases with dipolar interactions,[10,24] experimental realization of exotic condensed matter Hamiltonians with polar molecules confined in an optical lattice,[12] architectures for manipulating quantum information,[7–9] and creation of self-assembled dipolar crystals.[25]

These proposals typically require molecules with large dipole moments in a gas with relatively high density (small inter-particle separation) and ultralow temperature. The highest densities and lowest temperatures are achieved for gases that are quantum degenerate. In particular, in a Bose–Einstein condensate of polar molecules, even a relatively small dipole moment is sufficient to realize a situation where the dipole–dipole interaction strength far exceeds the kinetic energy. More generally, the quantum degeneracy of a gas can be characterized

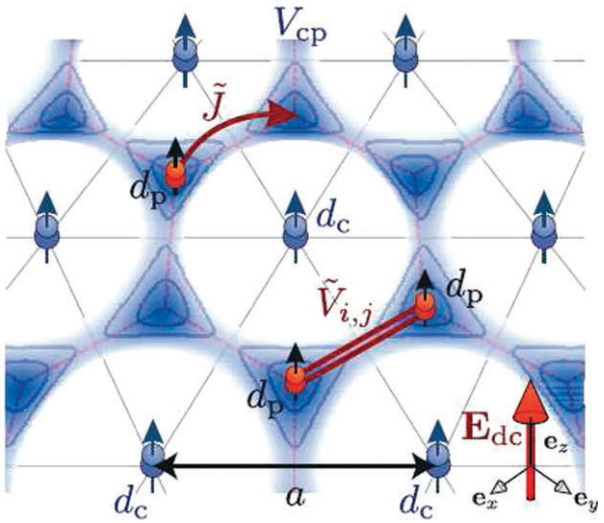

Fig. 2 Self-assembled dipolar crystal. Polar molecules confined in a 2D geometry have repulsive interactions when polarized perpendicular to the 2D plane. When the repulsive interaction is strong, the polar molecules can form a crystal. This crystal provides a new experimental tool for studying exotic condensed-matter Hamiltonians. Figure adapted with permission from G. Pupillo, A. Griessner, A. Micheli, M. Ortner, D.-W. Wang and P. Zoller, *Phys. Rev. Lett.*, 2008, **100**, 050402. Copyright 2008, American Physical Society.

by its phase-space density, PSD = $n\Lambda^3$ where n is the peak density and Λ is the thermal de Broglie wavelength. For a quantum degenerate gas, PSD $\geq$ 1. For a given gas temperature and density, the size of the dipole moment sets the interaction strength and in general, one wants a larger dipole moment to more easily observe interaction effects. As an extreme example in the strongly interacting limit, it is predicted that a gas of polar molecules confined in a two-dimension pancake geometry can form a dipolar crystalline phase (see Fig. 2).[25,26] For a gas density of 10^{12} cm^{-3} and molecular mass of about 100 amu (atomic mass unit), this crystalline phase requires that the dipole moment be greater than 3 Debye.[25]

III. Production of cold/ultracold polar molecules

Experimental efforts aimed at producing cold and ultracold polar molecules have generally followed two different approaches: one is to directly cool molecules to ultralow temperature; the other is to start from ultracold atoms, and then associate them into tightly bound molecules. The current status of experimental efforts is summarized in Table 1 where examples of results for different cooling methods are presented. The last row in Table 1 illustrates results from our recent creation of a high phase-space-density gas of KRb molecules.

A Direct cooling of molecules

The most straightforward approach for producing ultracold polar molecules would simply be to cool them directly to ultralow temperatures, just as is done for ultracold atomic gases. However, the powerful technique of laser cooling,[27] which launched experimental investigation of ultracold atomic gases, is much more problematic for molecules due to complex internal state structure. The basic issue is that achieving low

temperature necessitates momentum recoil accumulated from thousands to millions of excitation and spontaneously emitted photons. This in turn requires efficient cycling in a "closed" 2 or 3 level system, which is generally not feasible in electronic excitation of molecules. Recently, laser cooling of molecules *via* coherent scattering inside high-finesse optical cavities has been proposed,[8,28–30] but a necessary ingredient for successful implementation is an initial sample of cold molecules with a sufficiently high density to enable collective effects.[30] Free space laser cooling has also been proposed,[31] including the possibility of constructing a general purpose magneto-optic trap for a certain class of polar molecules.[32]

Two general molecule cooling techniques have been developed over the last 10 years that have proved to be very successful in producing a diverse set of cold polar molecules, including but not limited to CaH, CaF, OH, NH_3, ND_3, H_2CO, NH, PbO and YbF. These so-called "direct cooling" techniques include imbedding and cooling molecules in a cryogenically cooled helium buffer gas[33–35] and slowing molecules from a supersonic jet through Stark deceleration.[36,37] Direct cooling of polar molecule gases provides access to temperatures in the range of 10s to 100s of mK, which is sufficiently cold to allow molecules to be confined in electro-static,[38] AC electric field,[39] and magnetic traps.[34,40] These cold species can be used for precision measurements,[3] collisional studies,[37,41,42] and cold chemistry.[6,43] Other techniques being developed include magnetic[44,45] or optical deceleration[46] of molecular beams, velocity filtering of a molecular beam,[47] production of cold molecules *via* kinematic collisions,[48] or backward motion of a molecular beam source nozzle.[49] Despite the above range of methods being explored, however, none have successfully cooled molecules to below a few milliKelvin.[50] To further reduce the molecular temperature, methods such as the proposed laser cooling approaches discussed above, collisional cooling *via* evaporation, or sympathetic cooling with ultracold atoms might prove to be viable. Two preconditions for their success will be: (i) a favorable ratio of elastic and inelastic collisions; and (ii) a sufficiently dense sample of molecules accumulated inside a trap.[34] With further improvements that permit lower temperatures and higher trapped gas densities, it looks promising for dipole-dependent cold collision dynamics in directly cooled polar molecule gases to be accessible for study in the near future.

B Photo-association

An alternative to directly cooling polar molecules is to start from ultracold atoms and convert them pairwise into deeply bound molecules. This takes advantage of the fact that atoms can be laser cooled to temperatures of 100 μK or below. However, the challenge here is two fold: (i) to efficiently bring the atoms together to form tightly bound molecules and yet (ii) avoid any heating of the gas due to the release of the chemical binding energy. For a sense of the magnitude of the challenge, note that the binding energy for a typical alkali dimer in its rovibrational ground state is nine or more orders of magnitude larger than the kinetic energy of particles in an ultracold gas. For example, the binding energy of KRb molecules in their lowest energy state corresponds to a temperature of 6000 Kelvin, *i.e.* 6 billion times hotter than typical ultracold temperatures of <1 μK (Fig. 3). A general class of strategies that has been pursued to circumvent this dilemma is to perform the transfer in two steps, first (i) forming highly delocalized molecules by laser and/or magnetic fields, and then (ii) using either spontaneous or stimulated emission to transfer the excited state population into the ground state. We consider applications of these methods in more detail below.

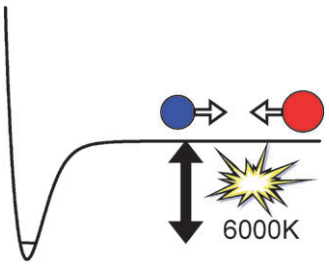

Fig. 3 Forming ultracold molecules from ultracold atoms is challenging because a large binding energy is released when two atoms form a tightly bound molecule. For example, the binding energy of rovibrational ground-state KRb molecules corresponds to a temperature of 6000 K (4000 cm^{-1}), which is 10^{10} times larger than a typical temperature of an ultracold atom gas.

One successful approach has been based on converting atom pairs into molecules by photo-association,[51] where one uses laser light to drive a transition between a scattering state of two atoms and an electronically excited molecular state. The electronically excited molecules can then quickly decay by spontaneous emission to form electronic ground-state molecules. The key advantage of such an optical process, as opposed to, for example, collisional formation of molecules, is that the binding energy is removed from the system as the difference between the absorbed and emitted photon energies, rather than being released as kinetic energy to heat the ultracold gas. In photo-association, only a small amount of heating remains due to the recoil of the resulting molecule as it emits a spontaneous photon. In favorable cases, however, this heating can correspond to a temperature increase of less than 1 μK.

Use of photo-association to make ultracold polar molecules in their rotational, vibrational, and electronic ground state was first demonstrated by Sage *et al.*[52] In their experiment, optical fields were applied to transfer Rb and Cs atoms in a continuum of scattering states to the absolute ground state of the RbCs molecule using the two steps illustrated in Fig. 4. A two-step process was necessary because of the extremely small wavefunction overlap between two free atoms and a tightly bound molecule. For example, at a density of 10^{10} cm^{-3}, which is typical for laser cooled atom gases, the typical distance between two neighboring atoms is $90\,000a_0$. In contrast, a tightly bound diatomic molecule might have an internuclear separation of $10a_0$ or less. As result of a distribution of Franck–Condon factors, the process is generally inefficient at forming a specified target quantum state.

The first step used by Sage *et al.* was photo-association followed by spontaneous decay to produce large, weakly bound electronic ground-state molecules in the lowest electronic triplet manifold but in very high vibrational (high-v) states.

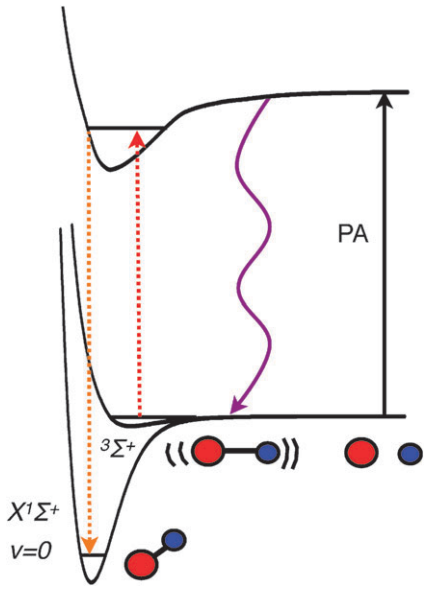

Fig. 4 Schematic of a two-step optical transfer process described in Sage *et al.*[52] that produced RbCs in the absolute ground state from laser-cooled Rb and Cs atoms. The first step is to create weakly bound molecules (in high vibrational levels) by photo-associating (PA) atoms into excited-state molecules that then decay back to the ground electronic state by spontaneous emission (wiggly line). These weakly bound molecules provide a better wave function overlap for the second transfer step to the absolute ground state. The second step uses a stimulated emission pump–dump process (dashed arrows) to enhance optical transfer from weakly bound molecules to the absolute ground state. Typically each iteration of this two-step process created 10 molecules in the absolute ground state when starting from 10^8 atoms.

In the spontaneous decay many high-v levels of the triplet ground state were populated, with the biggest branching ratio being 7% into $v = 37$.[52] The second step was then to apply two laser fields for a pump–dump transfer process using absorption and stimulated emission. This step transferred molecules in the $v = 37$ of the triplet ground-state to $v = 0$ of the singlet ground-state through an intermediate electronic excited state.

This technique did produce molecules in the absolute ground state at the temperature of 100 μK in their translational motion. However, the formation process in this proof-of-principle experiment was rather inefficient. Specifically, each laser pulse sequence produced only 10 absolute ground-state molecules from the initial 10^8 atoms. In addition, molecules in many other higher energy vibrational and rotational levels were produced at the same time. Nevertheless, this experiment highlights one general scheme as well as the challenges in converting ultracold atoms into tightly bound molecules. Other experiments have used photo-association of laser-cooled atoms to create ultracold polar molecules in bialkali systems such as KRb,[53,54] NaCs,[55] and LiCs.[56]

Although such an incoherent process based on spontaneous emission can never produce molecules populating only a single target state, it does provide useful guidance for how to improve the efficiency of photo-association methods for forming deeply bound ground-state molecules. One obviously desires to have enhanced transition rates driving both (i) initial excitation from the scattering atom states to a suitable excited molecular state as well as (ii) decay to a deeply bound vibrational level in the electronic ground potential. While optimization of the overall efficiency is limited by the molecular structure, techniques and proposals have emerged to enhance the transition strengths using accidental resonances between molecular states, either in the excited electronic potentials[57,58] or in the ground potential.[56] A recent proposal suggests that simply performing photo-association of atoms near a Fano–Feshbach resonance (discussed in section III.C) is sufficient to drive them into a deeply bound molecular state either through one-photon or two-photon transitions.[59,60] Although resonant-assisted photo-association enhances the transition rate by orders of magnitude, the overall transition rate is still rather weak, and using either one-photon or two-photon processes to drive atoms to a deeply bound state still appears challenging. An additional issue with this approach is that the initial state is a scattering state, and the time scale for two atoms to come close enough to be photo-associated, which can be of order a few ms, can effectively limit the transition Rabi rate for population transfer. As an important corollary, however, this implies that enhancing the phase-space density of the initial atomic gas can dramatically enhance the initial transition rate to form weakly associated molecules.

C Fully coherent scheme

One extremely powerful solution to the efficiency challenges outlined above is to have each transfer step remain fully coherent (and therefore even reversible) processes. In recent work we used a coherent transfer scheme to produce a near quantum degenerate gas of ultracold polar molecules in their rovibrational singlet ground state.[13] As opposed to the experiments discussed in the previous section, we start with an ultracold atom gas at a high phase-space density (PSD $\sim$ 1). This high phase-space density is achieved using the now standard cooling techniques of laser cooling followed by forced evaporation.[61,62] At the end of the evaporation, we have a quantum degenerate gas of K and Rb atoms, each in a single hyperfine state, at a temperature of several hundred nK. The atoms are confined in a far-detuned optical dipole trap, which can also confine the resulting KRb molecules.

We then use two coherent steps for production of ultracold polar molecules. First, we use a magnetic-field tunable scattering resonance, called a Fano–Feshbach resonance, to convert atoms pairwise into molecules. This is basically due to an adiabatic magnetic-field induced avoided curve crossing between free atom (K and Rb) states and a single, highly vibrationally excited state of the KRb molecule at the dissociation limit. Since the initial phase-space density of the quantum degenerate gas is high, a large fraction of the atoms can be converted into molecules in a single quantum state. Secondly, these extremely weakly bound molecules are then optically transferred into the rovibrational ground state using a two-photon coherent process. The basic approach of making molecules near a Fano–Feshbach resonance followed by coherent optical manipulation of the molecules' internal state has also been used recently to produce ultracold gases of homonuclear

(*i.e.*, non-polar) molecules.[63,64] In the next two sections, we discuss in more detail the two steps in this transfer that makes it possible to map the high phase-space density of an ultracold atomic gas into tightly bound polar molecules in the ultracold regime.

IV. Weakly bound Feshbach molecules

A Method

Fano–Feshbach resonances are scattering resonances that allow experimenters to control interactions in a quantum gas of atoms.[65,66] This powerful tool has played a key role in a number of exciting developments in ultracold atom gases, such as realization of the BCS–BEC crossover in Fermi gases,[67] the controlled collapse of a BEC,[68] and the observation of bright matter wave solitons.[69] As illustrated in Fig. 5a, these resonances occur when the energy of a pair of atoms in one hyperfine scattering channel ($E \geq 0$) is the same as the energy of a molecular bound state in a different hyperfine channel. Because the molecule and the pair of free atoms can have different magnetic moments, atom scattering can be tuned in and out of resonance using precisely controlled magnetic fields. This allows atom pairs to be converted into weakly bound molecules by adiabatically sweeping the magnetic field across the resonance (Fig. 5b).[17] The molecules that are created are extremely weakly bound and, moreover, their binding energy and size depend on the magnetic-field detuning from resonance. These exotic species, which only exist near the resonance, are often referred to as ''Feshbach molecules''. Their typical binding energy at magnetic fields near the resonance is on the order of $h \times 10$ kHz to $h \times 10$ MHz. Because these are very large, very high-v molecules, their permanent electric dipole moment is negligible; for example, the KRb Feshbach molecule has a calculated dipole moment that is of order 10^{-11} D.[70]

Magneto-association in a near quantum degenerate atomic gas is adiabatic, coherent, and efficient. For homonuclear dimers, the conversion efficiency from free atoms to Feshbach molecules has already been demonstrated to be near unity for quantum degenerate gases of alkali atoms.[71] However, to make polar ground-state molecules, heteronuclear dimers are of course required. Specifically, for KRb Feshbach molecules, we observe a maximum conversion efficiency from atoms to molecules of 25%.[72] This conversion efficiency, which is lower than the maximum value demonstrated for homonuclear Feshbach molecules, is affected by several factors.[72,73] To have a high conversion efficiency, high phase-space density is desired.[71] However, we convert Feshbach molecules from a mixture of fermionic K and bosonic Rb. As the phase-space density increases, the Rb cloud shrinks while the K cloud size remains relatively unchanged due to the Pauli pressure. This reduces the spatial overlap of the two clouds, therefore, the conversion efficiency drops. In addition, because of the mass difference between K and Rb, gravity causes an offset of the equilibrium positions of the two clouds in an optical trap. Finally, strong inelastic collisions on the time scale of the population transfer can also limit the conversion. For example, our experiment generates KRb molecules in a far-detuned optical dipole trap that confines both atoms and molecules, for which we observe a Feshbach molecule lifetime of 7 ms.[73] This is likely due to inelastic collisions that vibrationally quench the very high-v Feshbach molecules and result in a large energy release and loss of the molecules from the trap. Formation of heteronuclear Feshbach molecules has also been explored for LiK[74] as well as for another isotope of KRb.[75]

The fact that the Feshbach molecules are extremely weakly bound, and therefore very large, helps make the magneto-association efficient. However, we now want to coherently manipulate the molecules' internal state to reach a deeply bound level with a small internuclear spacing for a significant electric dipole moment. It is worth noting in this next step that even though the Feshbach molecules are unusually large dimers, the magneto-association step nevertheless has effectively reduced the mean internuclear separation from a few tens of thousand a_0 in the initial ultracold atom gas down to only a few hundred a_0 for the resulting molecules. This greatly facilitates further molecular state manipulation by providing a much larger Franck–Condon overlap to deeply bound states.

B Enhancement factor

The importance of this first step of magneto-association can be seen in a measured enhancement of the optical excitation rate. In Fig. 6, we show the loss rate of atoms or molecules as we apply laser light to drive transitions to an electronically excited molecular state, which then rapidly decays and leaves the trap. The excited state for this measurement is the same one we use

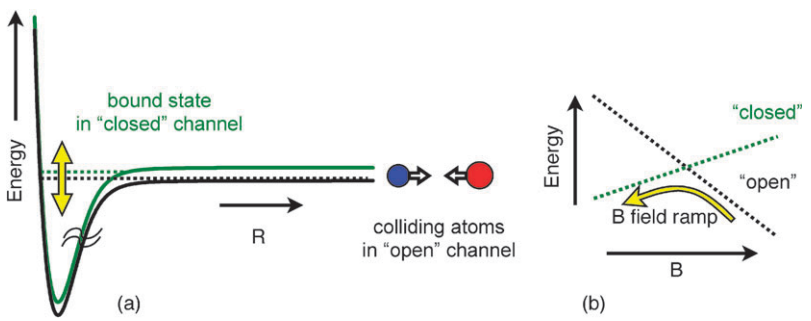

Fig. 5 (a) A Fano–Feshbach resonance occurs when the energy of a pair of atoms in one hyperfine (''open'') channel is the same as a molecular bound state in a different hyperfine (''closed'') channel. The system can be tuned into and out of resonance by changing the strength of an applied external magnetic field. (b) An appropriate magnetic-field ramp (the arrow) across a Fano–Feshbach resonance can adiabatically convert pairs of atoms into weakly bound Feshbach molecules. (Energy levels are not drawn to scale).

for coherent optical transfer to the absolute ground state, as described in the next section. In Fig. 6a, we show the loss rate of Feshbach molecules when driving the bound–bound transition, which when fit to an exponential yields a removal lifetime of τ_m = 0.093(6) ms. For comparison, Fig. 6b shows the considerably slower loss (τ_a = 190(30) ms) of K and Rb atoms when driving the corresponding free-bound (*i.e.*, photo-association) transition at the same magnetic-field detuning from resonance. Scaled appropriately to laser power, the ratio of electronic excitation rates for Feshbach molecules *vs.* atoms is $\frac{1/\tau_m}{I_m}\Big/\frac{1/\tau_a}{I_a}$. The measured values indicate an enhancement factor of $\approx$5000, which reveals several orders of magnitude advantage when initiating the final population transfer step from a weakly bound *vs.* free atom precursor state.

C Detection

Before discussing the next step in creating absolute ground-state molecules, it is useful to consider molecule detection. In an ultracold atom experiment, one typically probes the gas using time-of-flight (TOF) absorption imaging. Here, the gas is suddenly released from the trap and then imaged after an expansion time (TOF) that is typically a few to a few tens of ms. For the imaging, a pulse of resonant laser light illuminates the expanded gas and a CCD camera records the shadow image of the cloud. The total number of atoms and their momentum distribution can be obtained from these images. For molecules, however, imaging, or even just detecting

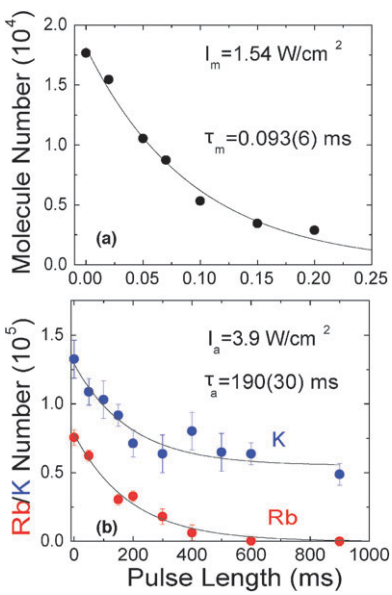

Fig. 6 Comparison of the optical excitation rate (a) from Feshbach molecules to the $v' = 23$ state of the excited $2^3\Sigma^+$ potential and (b) from a near quantum degenerate gas of atoms to the same excited state. The measured depletion of the molecule/atom population is due to excited KRb* formation followed by spontaneous decay and loss from the system. The KRb* formation rates were characterized by the exponential time scales, τ_m and τ_a, respectively. The enhancement factor for starting from Feshbach molecules instead of atoms near the Fano–Feshbach resonance is $\frac{\tau_a/I_a}{\tau_m/I_m} \approx 5000$.

molecules, with light absorption is much more challenging with the complicated internal state structure and lack of a clean two-level cycling transition.

However, an extremely useful feature of heteronuclear Feshbach molecules, which have only a tiny binding energy at magnetic fields near resonance, is that they can be imaged using the same photons as for the atomic cycling transition.[76] At an applied magnetic field of 546 G, which is less than 1 G detuned from a K–Rb resonance, KRb Feshbach molecules can be imaged using light resonant with the K atom cycling transition. When a molecule absorbs a photon, it dissociates, after which subsequent photons can scatter off the resulting free K atom. This gives a strong absorption signal, but does not distinguish between Feshbach molecules and any leftover unbound K atoms. To image only the Feshbach molecules, we apply an rf pulse that selectively drives unbound K atoms to a different hyperfine state, which at high magnetic field does not absorb the imaging light. In Fig. 7, we show a series of TOF absorption images of the ultracold Feshbach molecular gas. From these images, we determine that 4.5 $\times$ 10^4 Feshbach molecules are formed, at an expansion energy corresponding to a temperature of 330 nK. By perturbatively displacing the trap center and watching the ensuing ''sloshing'' motion of the cloud, we can verify that the Feshbach molecules are indeed confined in our far-detuned optical dipole trap as well as determine the trap parameters.[72]

Unfortunately, this detection technique cannot be directly applied to deeply bound molecules, such as KRb in its rovibrational ground state. However, by efficient coherent manipulation of the molecules' internal states, we can reversibly bring ground-state molecules back to the Feshbach state and then image them as Feshbach molecules. There are certainly other powerful laser methods for detecting and velocity map imaging ground-state polar molecules, based on, for example, resonant multiphoton ionization techniques. Direct absorption imaging of the ultracold molecular gas should also be possible. Nevertheless, this reversible coherent imaging process provides a good signal-to-noise level for KRb polar molecules, using techniques that are readily available and compatible with ultracold gas experiments.

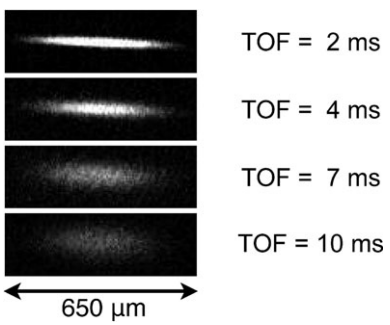

Fig. 7 A series of time-of-flight images for KRb Feshbach molecules at an applied magnetic field of 545.88 G. From images such as these we extract the total number (4.5 $\times$ 10^4) of molecules and the expansion energy (330 nK) of the molecular gas.

V. Two-photon optical transfer to absolute ground-state molecules

Once we have formed weakly bound Feshbach molecules by magneto-association, the second step is to use a coherent two-photon Raman technique to transfer these Feshbach molecules to the absolute rovibrational electronic ground state ($N = 0$, $v = 0$, of $X^1\Sigma^+$). In this section, we will see that the efficiency for such a coherent transfer process can be remarkably good (>90%).

A Three-level system

Fully coherent state manipulation is the key to efficient transfer of Feshbach molecules into the lowest energy rovibrational ground state without heating the ultracold gas. For the coherent population transfer to work well, we need both the upward ("pump") and downward ("dump") transitions to have reasonably good oscillator strengths. If the transitions are weak, high laser intensities are required and this will in general induce nonlinear effects that limit the conversion efficiency. A proposed solution is to use a carefully designed train of coherent pulses that can achieve complete population transfer to a single target state *via* coherent accumulation of well-understood weak-field effects.[77] This conversion process by a coherent pulse train is equivalent to a coherent STImulated Raman Adiabatic Passage (STIRAP) process[78] in a piece-wise manner.[79] However, this turns out to be unnecessary for alkali dimers, since one can in general find a single excited electronic intermediate state with relatively strong transition strengths with respect to both the initial Feshbach state and the final absolute ground state. The optimum transition strengths are obtained for an excited molecule state that has good overlap between its classical inner and outer turning points and the respective Condon points for both the upward and downward transitions. In addition, the intermediate state must have sufficient singlet–triplet mixing to couple Feshbach molecules, which are primarily triplet, to the final rovibrational ground state, which is of nearly pure singlet character.[52,80]

An appropriate choice of the electronically excited molecular state allows a pair of continuous-wave lasers to be used for a single-step STIRAP process that accesses the molecule's absolute ground state. Once the two lasers are properly stabilized, the long lifetimes of the initial and final states ensure that the transfer process is very efficient and reaches a single rovibrational state ($N = 0$, $v = 0$ of $X^1\Sigma^+$). Furthermore, due to the fully coherent nature of the optical transitions, the transfer avoids any heating due to photon recoil. Our transfer technique uses three molecular states, labelled $|i\rangle$, $|e\rangle$, and $|g\rangle$, that are coupled together by two laser fields with Rabi frequencies, Ω_1 and Ω_2, as shown in the inset of Fig. 8. Since the excited state $|e\rangle$ is lossy and short-lived, we introduce a decay rate γ. In general, states $|i\rangle$ (the Feshbach molecule state) and $|g\rangle$ (the absolute ground state for KRb molecules) can also decay, but this will be ignored since the time scale is much longer than the transfer process under consideration. The simplified Hamiltonian of the system in the basis

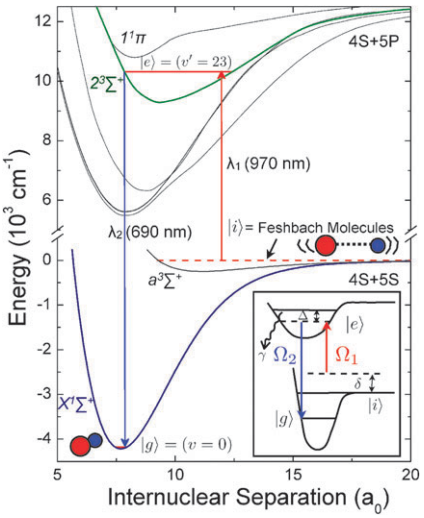

Fig. 8 Schematic of the transfer from KRb Feshbach molecules to the absolute rovibrational electronic ground state. The intermediate state was chosen to be the $v' = 23$ state of the nominally $2^3\Sigma^+$ electronically excited potential for its good wavefunction overlap to both the Feshbach molecules and the absolute ground-state molecules. The three levels are coupled by two lasers that have the laser wavelength of λ_1 (970 nm) and λ_2 (690 nm) and are both referenced to a stable optical frequency comb. (Inset) Diagram showing the parameters that describe a coupled three-level system, where Ω_1 and Ω_2 describe Rabi frequencies for the two transitions.

set of $|i\rangle$, $|e\rangle$, and $|g\rangle$, after making the rotating-wave approximation, is

$$H = \frac{\hbar}{2}\begin{bmatrix} 0 & \Omega_1(t) & 0 \\ \Omega_1(t) & 2\Delta - i\gamma & \Omega_2(t) \\ 0 & \Omega_2(t) & 2\delta \end{bmatrix}, \qquad (1)$$

where Δ denotes the one-photon detuning and δ denotes the two-photon detuning, as shown in the inset to Fig. 8. When the Raman resonance condition is met, namely $\delta = 0$, one of the eigenstates of the system is $\cos\theta|i\rangle + \sin\theta|g\rangle$, where $\theta = \tan^{-1}(\frac{\Omega_1(t)}{\Omega_2(t)})$. This state is dark in that it is not coupled to the lossy $|e\rangle$ level. This dark state is important because it allows, with an appropriate time dependence of the applied coupling fields $\Omega_1(t)$ and $\Omega_2(t)$, the full population of $|i\rangle$ to be converted to $|g\rangle$ without ever populating the lossy excited state $|e\rangle$. The process of STIRAP provides fully coherent transfer between states $|i\rangle$ and $|g\rangle$.[78] It is important to note that we have assumed that there is a well-defined phase relation between the two coupling fields. This assumption sets a demanding challenge for experiments by requiring that the two Raman lasers, which in our case are at very different wavelengths, remain phase coherent during the time scale relevant for adiabatic transfer.

For the creation of absolute ground-state KRb molecules, the wavelengths of the cw coupling lasers are 970 nm (λ_1) and 690 nm (λ_2). The KRb potentials and the states relevant for our transfer scheme are shown in Fig. 8. In our experiment, the two-photon beat can be maintained to a few kHz linewidth by referencing each laser to a stable optical femtosecond comb.[81] The few kHz linewidth means that the STIRAP transfer must be completed in a time less than a few hundred μs. This is only

possible if the intermediate state has a sufficiently large transition dipole moment both to the Feshbach molecule state, $|i\rangle$, and to the deeply bound final states, $|g\rangle$. In our experiment, we used the vibrationally excited $v = 23$ level of the nominally $2^3\Sigma^+$ electronically excited molecular potential.[13,82] This state has a small mixing with a nearby $1^1\Pi$ state, which is necessary to couple to the $^1\Sigma^+$ absolute ground state. The upward transition dipole moment from the Feshbach molecule state to this intermediate state was determined to be 0.013 Debye, where this transition dipole moment already includes the Franck–Condon factor arising from wavefunction overlaps.

B Two-photon spectroscopy

Before performing STIRAP to coherently transfer population from the Feshbach molecule state to the absolute ground state, we first need to precisely determine the energy of absolute ground state. We did this using two-photon spectroscopy methods described below. In addition, by adding an applied electric field, this spectroscopy provided a measurement of the electric dipole moment of the absolute ground-state molecules. Recall that there exists a dark state, as discussed above, $\cos\theta|i\rangle + \sin\theta|g\rangle$ where $\theta = \tan^{-1}(\frac{\Omega_1(t)}{\Omega_2(t)})$, when the two-photon Raman resonance condition is fulfilled. In the limit of $\Omega_2 \gg \Omega_1$, the dark state becomes $|i\rangle$, and therefore no loss is expected for $|i\rangle$ when $\delta = 0$. To search for the absolute ground state, we fixed the frequency of the laser corresponding to λ_1 (Rabi frequency of Ω_1) to resonantly drive Feshbach molecules to the electronically excited intermediate state discussed previously. Then we scanned the λ_2 laser frequency (Rabi frequency of Ω_2) and monitored the population of the Feshbach molecules, $|i\rangle$, after pulsing on both lasers. Fig. 9 shows the two-photon spectroscopy results. In the absence of Ω_2, the Feshbach molecules disappear because they are resonantly excited by the Ω_1 laser field. These excited molecules will spontaneously decay and be lost from the trap as well as from our signal, which comes exclusively from the weakly bound Feshbach molecules. However, when the second laser field, Ω_2, is turned on and the Raman resonance condition is fulfilled, $\delta = 0$, the Feshbach molecules remain due to the formation of the dark state. From this measurement, the exact binding energy of the absolute ground state was precisely determined to be $h \times 125.319703$ THz (4180.22 cm^{-1}) at 545.88 G.[13]

Knowing the energy of the absolute ground state, $|g\rangle$, we can characterize the coupling strength Ω_2. Here, we fix the corresponding laser frequency of λ_2 on resonance ($\Delta = 0$) and scan the corresponding laser frequency of λ_1. The inset of Fig. 9 shows the measured population of the Feshbach molecule state, $|i\rangle$, after the two-color laser pulse. The frequency splitting between the two minima corresponds to the Rabi frequency of the $|g\rangle$ to $|e\rangle$ transition driven by Ω_2. For this data, the 7 MHz Rabi frequency was obtained using 6 mW of laser power focused to a 40 μm beam waist; this yields a transition dipole moment of 0.03 D for the intermediate to ground-state transition.

This form of two-photon spectroscopy can also be used to map out the energy splitting of states $|i\rangle$ and $|g\rangle$ as a function of an applied electric field. In the case where the initial state $|i\rangle$ has a negligible dipole moment, such as a Feshbach molecule, the measured Stark shift comes solely from the final state $|g\rangle$. Fig. 10 shows the measured Stark shift for rovibrational ground-state KRb molecules. To determine the electric dipole moment of $|g\rangle$, we also need to know the rotational constant, since the resultant polarization in an electric field arises from mixing opposite parity rotational levels (predominantly with $N = 1$ for our $N = 0$ level) of the $^1\Sigma^+$ molecules. We extracted a rotational constant of $B = 1.1139$ GHz by independently measuring the location of the $N = 2$ state using two-photon spectroscopy, which is $6B$ above the $N = 0$ state. Finally, from the Stark shift of the $N = 0$ molecule state (Fig. 10) and the measured rotational splitting, we find that the permanent electric dipole moment is 0.566 D.[13]

C Transfer

We use STIRAP[78] to transfer KRb Feshbach molecules into the absolute ground state. As discussed above, the population of $|i\rangle$ can be adiabatically transferred to $|g\rangle$ by an appropriate choice for the time dependence of the coupling laser fields $\Omega_1(t)$ and $\Omega_2(t)$. The counter-intuitive STIRAP pulse sequence is to turn on Ω_2 first, and then ramp down Ω_2 (by lowering the laser intensity) while ramping up Ω_1 (see Fig. 11a). At the end of the STIRAP transfer, Ω_1 can be turned off. By the designed time sequence, the dark state evolves from the initial to the final state. And therefore, all of the Feshbach molecules can in principle be transferred to the absolute ground state without

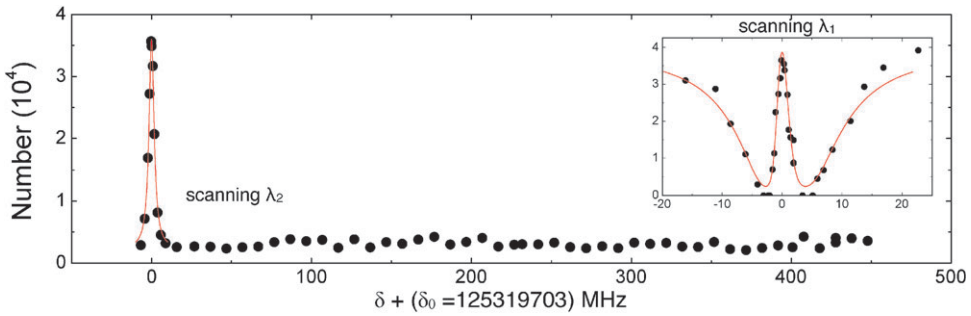

Fig. 9 Finding the absolute ground-state level ($N = 0$, $v = 0$ of $X^1\Sigma$) of KRb. The binding energy of the absolute ground state was identified using two-photon dark resonance spectroscopy, where the laser frequency of λ_1 (defined in Fig. 8) was fixed and the frequency of λ_2 was scanned. δ is the two-photon detuning relative to the energy of the initial $|i\rangle$ and the final state $|g\rangle$, which are separated by $\delta_0 = 125319703$ MHz. (Inset) This Figure has the same axes as the main Figure. The coupling strength Ω_2 was determined by measuring the dark resonance splitting at the fixed λ_2 laser frequency while the λ_1 laser frequency was scanned.

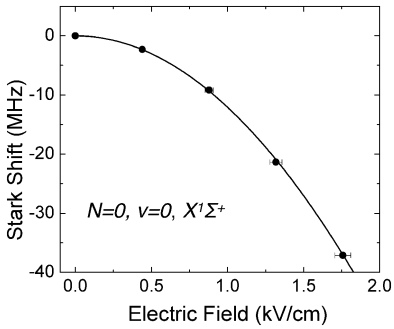

Fig. 10 Stark spectroscopy. The measured Stark shift of the rovibrational electronic ground state of KRb is shown. From the measured Stark shift and using the rotational constant extracted from the measured energy difference between the $N = 0$ and $N = 2$ levels at zero field, we found the $v = 0$ KRb permanent electric dipole moment to be 0.566 D.[13]

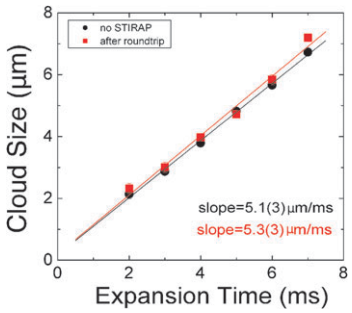

Fig. 12 From a series of TOF images (see also Fig. 7), we can measure the expansion energy of Feshbach molecules before and after a round-trip transfer to the absolute ground state. Within their uncertainty, the two measurements give the same gas expansion velocity; thus there is no observable heating during the STIRAP transfer process.[83]

ever populating the lossy intermediate state $|e\rangle$. This means that there is no spontaneous emission and the state transfer is fully coherent. Without spontaneous emission, there should also be no heating of the molecule gas in the transfer. However, there can remain a small momentum recoil of the molecules caused by the two-photon Raman process, which can be minimized by having the two laser beams for STIRAP be co-propagating. With this configuration for our KRb transfer, the calculated momentum kick corresponds to a temperature increase of only 13 nK.

Fig. 11b shows STIRAP transfer of KRb from the weakly bound Feshbach molecule state to the absolute ground state. Since we only detect population in the initial Feshbach molecule state, we also perform a reverse STIRAP pulse sequence to bring the deeply bound molecules back to Feshbach molecules for detection. This non-standard molecule detection method works surprisingly well because the STIRAP transfer can be very efficient and because absorption imaging of the Feshbach molecule gas has good signal-to-noise, similar to that typically obtained in ultracold atom gas imaging. As seen in Fig. 11b, the round-trip transfer here has an efficiency of 67%. Assuming equal efficiency each way, the one-way STIRAP transfer efficiency is 81%. Under optimal conditions, we have observed one-way efficiency of >90%. Fig. 12 shows a measurement of the molecular gas temperature using time-of-flight absorption imaging for Feshbach molecules before and after round-trip STIRAP transfer, which illustrates no measurable heating observed in the transfer process.[83] Under optimal conditions, one-way STIRAP yields 4.6×10^4 KRb polar molecules in their absolute ground state at a temperature of 350 nK. The molecules are trapped and have a peak number density of 10^{12} cm^{-3}, corresponding to a phase-sapce density ≈ 0.02.

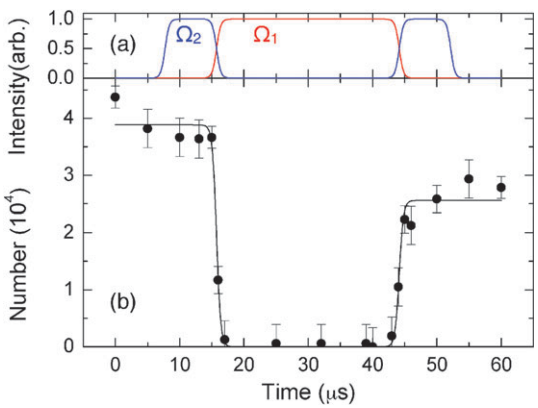

Fig. 11 (a) Intensity *vs.* time for the round-trip STIRAP pulse sequence. The actual transfer step (ramping down the intensity of one laser field while ramping up the other) takes 4 μs. (b) Initial state (Feshbach molecules) population during the STIRAP pulse sequence shown in (a). The initial state population vanishes after being transferred to the absolute ground state in the first 4 μs period when both coupling laster fields are on. To detect the ground-state molecules, a reversed STIRAP transfer (the second 4 μs period when both coupling laser fields are on) is used to bring these molecules back to Feshbach molecules. Assuming equal transfer efficiency each way, the one-way STIRAP efficiency is 81%.[83]

VI. Outlook

With the production of absolute ground-state KRb molecules at 350 nK, we can begin to explore some of the topics touched upon in the introduction to this perspective, such as electric-field dependence of elastic and inelastic collisions, ultracold chemistry, and quantum gases of polar molecules. Our KRb molecule gas is already well into the regime of relatively high density and low temperature where one can explore collisional effects. An immediate question is what is the lifetime of the trapped ro-vibronic ground-state polar molecules and what, if any, collision processes affect this lifetime? While one might expect a long lifetime for ultracold ro-vibronic ground-state molecules, we have already seen preliminary evidence that inelastic atom–molecule collisions can cause rapid number loss in our optical dipole trap. Because the first step of Feshbach molecule creation is only 10 to 25% efficient, leftover atoms remain in the far-detuned optical dipole trap with the molecules. Using a combination of rf fields and resonant light to selectively drive atoms out of the trap, we can vary the number of leftover Rb and K atoms. Fig. 13 shows a measurement of the lifetime of the ground-state molecules with K atoms and

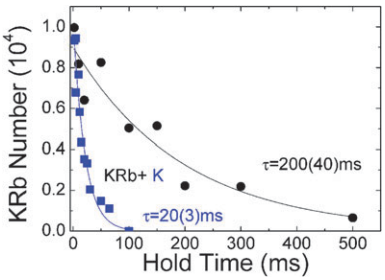

Fig. 13 The collisional stability of trapped KRb molecules is currently being investigated. Here, we show the measured KRb lifetime in the presence of no K atoms (circles) (from our detection limit, the K number is $<1 \times 10^3$) and 10^5 K atoms (squares). The observed KRb molecule lifetime, τ, is much shorter in the presence of K atoms (density $\sim 3 \times 10^{11}$ cm^{-3}). For these measurements, the Rb atom density was less than 10^9 cm^{-3}.

without K atoms. The number of molecules is measured after STIRAP transfer to absolute ground-state molecules, holding for a variable time, and then performing a reverse STIRAP back to the Feshbach molecule state for detection. In this measurement, observed loss of the molecules can correspond either to (i) trap loss or to (ii) a change in the molecules' internal state, since our detection relies on the ability to coherently bring the molecules back to the Feshbach molecule state. While this data shows clear evidence of inelastic collisions of K and KRb, it also raises many questions such as the mechanisms for this observed loss, where one possibility is chemical reaction (*i.e.*, K + KRb $\rightarrow$ K_2 + Rb) in the ultracold regime and another possibility is hyperfine state changing collisions, as well as what limits the lifetime of a pure gas of trapped molecules.

Obviously, another topic of immediate interest is dimer–dimer collisions, including their electric-field dependence. As can be seen in Fig. 10, the KRb molecule begins to be polarized (*i.e.* exhibit strong mixing between adjacent opposite parity N levels and thus yielding nearly linear Stark shifts) at relatively modest electric fields. For example, at an applied electric field of 8 kV cm^{-1}, KRb is 50% polarized with an effective dipole moment that is 0.28 D. Since the molecular gas is in the ultracold regime, the quantum statistics of the particles plays an important role. Our KRb molecules are fermions. For zero applied electric field, ultracold fermionic molecules prepared in a single internal state can only collide in an odd partial wave (because the two-particle wave function must be antisymmetric with respect to exchange). However, the lowest odd partial wave, p-wave, has a centrifugal barrier that can be much higher than the translational temperature of an ultracold gas. For example, for KRb the p-wave barrier height corresponds to a temperature of 16 μK[21] in zero electric field. Therefore, one predicts that the fermionic nature of our ultracold molecules will naturally protect them against inelastic and reactive self collisions. However, an interesting feature of polar molecules is that, in an applied electric field, the dipole–dipole interaction can effectively lower the centrifugal barrier,[18] and therefore the degree of collisional interaction and even cold chemistry can be controlled with an applied electric field for a pure molecular gas of KRb.

To explore the effects of quantum statistics it is important to be able to prepare the molecules in a single internal state. The STIRAP process, since it is fully coherent, should populate only the rovibrational ground state, and any molecules left in the Feshbach molecule state can be easily removed with resonant light. However, the nuclear spin degree-of-freedom gives rise to the possibility of molecules in different hyperfine states.[84,85] Understanding and controlling the hyperfine state of the molecules will be important for future experiments, including ultracold collisions of dipoles and schemes that may utilize hyperfine spins for quantum information.

Finally, the work described here will allow experiments to begin exploring the many proposed uses of quantum gases of ultracold polar molecules, such as for quantum information or simulation of condensed matter Hamiltonians. For our trapped gas of KRb ground-state molecules we estimate that $T/T_F = 2.5$ (PSD ≈ 0.02). Here, T_F is the Fermi temperature, which characterizes the temperature regime for quantum degeneracy of a gas of fermions. If the elastic and inelastic collision rates are favorable, the trapped molecule gas could be evaporatively cooled to a temperature below T_F to realize a dipolar Fermi gas and initiate experimental investigation of quantum gases of polar molecules with strong dipole–dipole interactions. Looking ahead, we also note that the two-step coherent transfer scheme we introduce here is very general and could be applied to other bi-alkali species. These species include ones that have significantly larger predicted dipole moments,[86] as well as ones that have different quantum statistics (bosons).

Acknowledgements

We thank J. Zirbel, A. Pe'er, M. Miranda, B. Neyenhuis, and D. Wang for their contributions to the work reported here. We thank S. Kotochigova, P. Julienne, G. Quéméner, and J. Bohn for their theoretical support. Funding support is provided by NSF and NIST. S. O. acknowledges support from the Alexander von Humboldt Foundation and K.-K. N. from NSF.

References

1 P. G. H. Sandars, *Phys. Rev. Lett.*, 1967, **19**, 1396–1398.
2 M. G. Kozlov and L. N. Labzowsky, *J. Phys. B: At., Mol. Opt. Phys.*, 1995, **28**, 1933–1961.
3 E. R. Hudson, H. J. Lewandowski, B. C. Sawyer and J. Ye, *Phys. Rev. Lett.*, 2006, **96**, 143004.
4 C. Ticknor and J. L. Bohn, *Phys. Rev. A: At., Mol., Opt. Phys.*, 2005, **72**, 032717.
5 A. V. Avdeenkov and J. L. Bohn, *Phys. Rev. Lett.*, 2003, **90**, 043006.
6 R. V. Krems, *Phys. Chem. Chem. Phys.*, 2008, **10**, 4079.
7 D. DeMille, *Phys. Rev. Lett.*, 2002, **88**, 067901.
8 A. Andre, D. DeMille, J. M. Doyle, M. D. Lukin, S. E. Maxwell, P. Rabl, R. J. Schoelkopf and P. Zoller, *Nat. Phys.*, 2006, **2**, 636–642.
9 S. F. Yelin, K. Kirby and R. Cote, *Phys. Rev. A: At., Mol., Opt. Phys.*, 2006, **74**, 050301.
10 M. A. Baranov, *Phys. Rep.*, 2008, **464**, 71.
11 L. Santos, G. V. Shlyapnikov, P. Zoller and M. Lewenstein, *Phys. Rev. Lett.*, 2000, **85**, 1791–1794.
12 G. Pupillo, A. Micheli, H. P. Büchler and P. Zoller, in *Cold molecule: creation and application*, ed. Roman V. Krems, William C. Stwalley, and Bretislav Friedrich, CRC, 2009, arXiv:0805.1896.

13 K.-K. Ni, S. Ospelkaus, M. H. G. de Miranda, A. Pe'er, B. Neyenhuis, J. J. Zirbel, S. Kotochigova, P. S. Julienne, D. S. Jin and J. Ye, *Science*, 2008, **322**, 231.
14 J. Stuhler, A. Griesmaier, T. Koch, M. Fattori, M. T. Pfau, S. Giovanazzi, P. Pedri and L. Santos, *Phys. Rev. Lett.*, 2005, **95**, 150406.
15 Th. Lahaye, T. Koch, B. Fröhlich, M. Fattori, J. Metz, A. Griesmaier, S. Giovanazzi and T. Pfau, *Nature*, 2007, **448**, 672.
16 T. Lahaye, J. Metz, B. Fröhlich, T. Koch, M. Meister, A. Griesmaier, T. Pfau, H. Saito, Y. Kawaguchi and M. Ueda, *Phys. Rev. Lett.*, 2008, **101**, 080401.
17 T. Köhler, K. Góral and P. S. Julienne, *Rev. Mod. Phys.*, 2006, **78**, 1311.
18 J. L. Bohn, M. Cavagnero and C. Ticknor, *New J. Phys.*, 2009, **11**, 055039.
19 A. V. Gorshkov, P. Rabl, G. Pupillo, A. Micheli, P. Zoller, M. D. Lukin and H. P. Büchler, *Phys. Rev. Lett.*, 2008, **101**, 073201.
20 L. Pitaevskii, in *Bose–Einstein Condensation in Atomic Gases*, ed. M. Inguscio, S. Stringari and C. E. Wieman, Proceedings of the International School of Physics "Enrico Fermi", Course CXL, IOS Press, Amsterdam, 1999, pp. 287–319.
21 *p*-Wave barrier was calculated from the C_6 coefficient between two KRb($v = 0$) molecules provided by S. Kotochigova, oral presentation, 39th annual meeting of Division of Atomic, Molecular and Optical Physics, American Physical Society, 2008.
22 C. Ticknor, *Phys. Rev. A: At., Mol., Opt. Phys.*, 2007, **76**, 052703.
23 M. Cavagnero and C. Newell, *New J. Phys.*, 2009, **11**, 055040.
24 T. Lahaye, C. Menotti, L. Santos, M. Lewenstein and T. Pfau, arXiv:0905.0386, 2009.
25 H. P. Büchler, E. Demler, M. Lukin, A. Micheli, N. Prokof'ev, G. Pupillo and P. Zoller, *Phys. Rev. Lett.*, 2007, **98**, 060404.
26 G. Pupillo, A. Griessner, A. Micheli, M. Ortner, D.-W. Wang and P. Zoller, *Phys. Rev. Lett.*, 2008, **100**, 050402.
27 S. Chu, *Rev. Mod. Phys.*, 1998, **70**, 685–706; C. N. Cohen-Tannoudji, *Rev. Mod. Phys.*, 1998, **70**, 707–719; W. D. Phillips, *Rev. Mod. Phys.*, 1998, **70**, 721–741.
28 P. Domokos and H. Ritsch, *Phys. Rev. Lett.*, 2002, **89**, 253003.
29 G. Morigi, P. W. H. Pinkse, M. Kowalewski and R. de Vivie-Riedle, *Phys. Rev. Lett.*, 2007, **99**, 073001.
30 B. L. Lev, A. Vukics, E. R. Hudson, B. C. Sawyer, P. Domokos, H. Ritsch and J. Ye, *Phys. Rev. A: At., Mol., Opt. Phys.*, 2008, **77**, 023402.
31 M. D. Di Rosa, *Eur. Phys. J. D*, 2004, **31**, 395.
32 B. K. Stuhl, B. C. Sawyer, D. Wang and J. Ye, *Phys. Rev. Lett.*, 2008, **101**, 243002.
33 J. D. Weinstein, R. deCarvalho, T. Guillet, B. Friedrich and J. M. Doyle, *Nature*, 1998, **395**, 148–150.
34 M. T. Hummon, W. C. Campbell, H. Lu, E. Tsikata, Y. Wang and J. M. Doyle, *Phys. Rev. A: At., Mol., Opt. Phys.*, 2008, **78**, 050702.
35 L. D. van Buuren, C. Sommer, M. Motsch, S. Pohle, M. Schenk, J. Bayerl, P. W. H. Pinkse and G. Rempe, *Phys. Rev. Lett.*, 2009, **102**, 033001.
36 H. L. Bethlem, G. Berden and G. Meijer, *Phys. Rev. Lett.*, 1999, **83**, 1558–1561.
37 B. C. Sawyer, B. K. Stuhl, D. Wang, M. Yeo and J. Ye, *Phys. Rev. Lett.*, 2008, **101**, 203203.
38 S. Y. van de Meerakker, P. H. Smeets, N. Vanhaecke, R. T. Jongma and G. Meijer, *Phys. Rev. Lett.*, 2005, **94**, 023004.
39 J. van Veldhoven, H. L. Bethlem and G. Meijer, *Phys. Rev. Lett.*, 2005, **94**, 083001.
40 B. C. Sawyer, B. L. Lev, E. R. Hudson, B. K. Stuhl, M. Lara, J. L. Bohn and J. Ye, *Phys. Rev. Lett.*, 2007, **98**, 253002.
41 K. Maussang, D. Egorov, J. S. Helton, S. V. Nguyen and J. M. Doyle, *Phys. Rev. Lett.*, 2005, **94**, 123002.
42 J. J. Gilijamse, S. Hoekstra, S. Y. T. van de Meerakker, G. C. Groenenboom and G. Meijer, *Science*, 2006, **313**, 1617.
43 E. R. Hudson, C. Ticknor, B. C. Sawyer, C. A. Taatjes, H. J. Lewandowski, J. R. Bochinski, J. L. Bohn and Jun Ye, *Phys. Rev. A: At., Mol., Opt. Phys.*, 2006, **73**, 063404.
44 S. D. Hogan, D. Sprecher, M. Andrist, N. Vanhaecke and F. Merkt, *Phys. Rev. A: At., Mol., Opt. Phys.*, 2007, **76**, 023412.
45 E. Narevicius, A. Libson, C. G. Parthey, I. Chavez, J. Narevicius, U. Even and M. G. Raizen, *Phys. Rev. Lett.*, 2008, **100**, 093003.
46 R. Fulton, A. I. Bishop, M. N. Shneider and P. F. Barker, *Nat. Phys.*, 2006, **2**, 465.
47 S. A. Rangwala, T. Junglen, T. Rieger, P. W. H. Pinkse and G. Rempe, *Phys. Rev. A: At., Mol., Opt. Phys.*, 2003, **67**, 043406.
48 M. S. Elioff, J. J. Valentini and D. W. Chandler, *Science*, 2003, **302**, 1940.
49 M. Gupta and D. Herschbach, *J. Phys. Chem. A*, 2001, **105**, 1626.
50 The work of F. M. Crompvoets, R. T. Jongma, H. L. Bethlem, A. J. A. van Roij and G. Meijer, *Phys. Rev. Lett.*, 2002, **89**, 093004, reports a molecular gas at a temperature of 250 μK, but with a much reduced number density.
51 K. M. Jones, E. Tiesinga, P. D. Lett and P. S. Julienne, *Rev. Mod. Phys.*, 2006, **78**, 483.
52 J. M. Sage, S. Sainis, T. Bergeman and D. DeMille, *Phys. Rev. Lett.*, 2005, **94**, 203001.
53 D. Wang, J. Qi, M. F. Stone, O. Nikolayeva, H. Wang, B. Hattaway, S. D. Gensemer, P. L. Gould, E. E. Eyler and W. C. Stwalley, *Phys. Rev. Lett.*, 2004, **93**, 243005.
54 M. W. Mancini, G. D. Telles, A. R. Caires, V. S. Bagnato and L. G. Marcassa, *Phys. Rev. Lett.*, 2004, **92**, 133203.
55 C. Haimberger, J. Kleinert, M. Bhattacharya and N. P. Bigelow, *Phys. Rev. A: At., Mol., Opt. Phys.*, 2004, **70**, 021402.
56 J. Deiglmayr, A. Grochola, M. Repp, K. Mörtlbauer, C. Glück, J. Lange, O. Dulieu, R. Wester and M. Weidemüller, *Phys. Rev. Lett.*, 2008, **101**, 133004.
57 C. M. Dion, C. Drag, O. Dulieu, B. Laburthe Tolra, F. Masnou-Seeuws and P. Pillet, *Phys. Rev. Lett.*, 2001, **86**, 2253.
58 A. J. Kerman, J. M. Sage, S. Sainis, T. Bergeman and D. DeMille, *Phys. Rev. Lett.*, 2004, **92**, 033004.
59 P. Pellegrini, M. Gacesa and R. Côté, *Phys. Rev. Lett.*, 2008, **101**, 053201.
60 E. Kuznetsova, S. F. Yelin, M. Gacesa, P. Pellegrini and R. Côté, *New J. Phys.*, 2008, **11**, 055028, arXiv:0812.3088.
61 E. A. Cornell and C. E. Wieman, *Rev. Mod. Phys.*, 2002, **74**, 875.
62 W. Ketterle, D. S. Durfee and D. M. Stamper-Kurn, in *Bose–Einstein Condensation in Atomic Gases*, ed. M. Inguscio, S. Stringari and C. E. Wieman, Proceedings of the International School of Physics "Enrico Fermi", Course CXL, IOS Press, Amsterdam, 1999, pp. 67–176.
63 F. Lang, K. Winkler, C. Strauss, R. Grimm and J. Hecker Denschlag, *Phys. Rev. Lett.*, 2008, **101**, 133005.
64 J. G. Danzl, E. Haller, M. Gustavsson, M. J. Mark, R. Hart, N. Bouloufa, O. Dulieu, H. Ritsch and H.-C. Nägerl, *Science*, 2008, **321**, 1062.
65 S. Inouye, M. R. Andrews, J. Stenger, H.-J. Miesner, D. M. Stamper-Kurn and W. Ketterle, *Nature*, 1998, **392**, 151.
66 C. Chin, R. Grimm, P. Julienne and E. Tiesinga, arXiv:0812.1496, 2008.
67 C. A. Regal and D. S. Jin, *Adv. At., Mol., Opt. Phys.*, 2006, **54**, 1–79.
68 J. L. Roberts, N. R. Claussen, S. L. Cornish, E. A. Donley, E. A. Cornell and C. E. Wieman, *Phys. Rev. Lett.*, 2001, **86**, 4211.
69 K. E. Strecker, G. B. Partridge, A. G. Truscott and R. G. Hulet, *Nature*, 2002, **417**, 150.
70 S. Kotochigova, P. S. Julienne and E. Tiesinga, *Phys. Rev. A: At., Mol., Opt. Phys.*, 2003, **68**, 022501.
71 E. Hodby, S. T. Thompson, C. A. Regal, M. Greiner, A. C. Wilson, D. S. Jin, E. A. Cornell and C. E. Wieman, *Phys. Rev. Lett.*, 2005, **94**, 120402.
72 J. J. Zirbel, K.-K. Ni, S. Ospelkaus, T. L. Nicholson, M. L. Olsen, P. S. Julienne, C. E. Wieman, J. Ye and D. S. Jin, *Phys. Rev. A: At., Mol., Opt. Phys.*, 2008, **78**, 013416.
73 J. J. Zirbel, K.-K. Ni, S. Ospelkaus, J. P. D'Incao, C. E. Wieman, J. Ye and D. S. Jin, *Phys. Rev. Lett.*, 2008, **100**, 143201.
74 A.-C. Voigt, M. Taglieber, L. Costa, T. Aoki, W. Wieser, T. W. Hänsch and K. Dieckmann, *Phys. Rev. Lett.*, 2009, **102**, 020405.
75 C. Weber, G. Barontini, J. Catani, G. Thalhammer, M. Inguscio and F. Minardi, *Phys. Rev. A: At., Mol., Opt. Phys.*, 2008, **78**, 061601.
76 C. Ospelkaus, S. Ospelkaus, L. Humbert, P. Ernst, K. Sengstock and K. Bongs, *Phys. Rev. Lett.*, 2006, **97**, 120402.
77 A. Pe'er, E. A. Shapiro, M. C. Stowe, M. Shapiro and J. Ye, *Phys. Rev. Lett.*, 2007, **98**, 113004.

78 K. Bergmann, H. Theuer and B. W. Shore, *Rev. Mod. Phys.*, 1998, **70**, 1003–1025.
79 E. A. Shapiro, A. Pe'er, J. Ye and M. Shapiro, *Phys. Rev. Lett.*, 2008, **101**, 023601.
80 W. C. Stwalley, *Eur. Phys. J. D*, 2004, **31**, 221.
81 S. T. Cundiff and J. Ye, *Rev. Mod. Phys.*, 2003, **75**, 325.
82 S. Kotochigova, E. Tiesinga and P. S. Julienne, *New J. Phys.*, 2009, **11**, 055043.
83 S. Ospelkaus, K.-K. Ni, M. H. G. de Miranda, B. Neyenhuis, D. Wang, S. Kotochigova, P. S. Julienne, D. S. Jin and J. Ye, *Faraday Discuss.*, 2009, **142**, 351, DOI: 10.1039/b821298h.
84 J. Aldegunde, B. A. Rivington, P. S. Zuchowski and J. M. Hutson, *Phys. Rev. A: At., Mol., Opt. Phys.*, 2008, **78**, 033434.
85 P. Julienne, *Faraday Discuss.*, 2009, **142**, 361arXiv0812.1233.
86 J. Deiglmayr, M. Aymar, R. Wester, M. Weidemüller and O. Dulieu, *J. Chem. Phys.*, 2008, **129**, 064309.